9/12/86

(19)

UCID-20785

INDUCTION LINACS AS RADIATION PROCESSORS

Daniel L. Birx

April 14, 1986

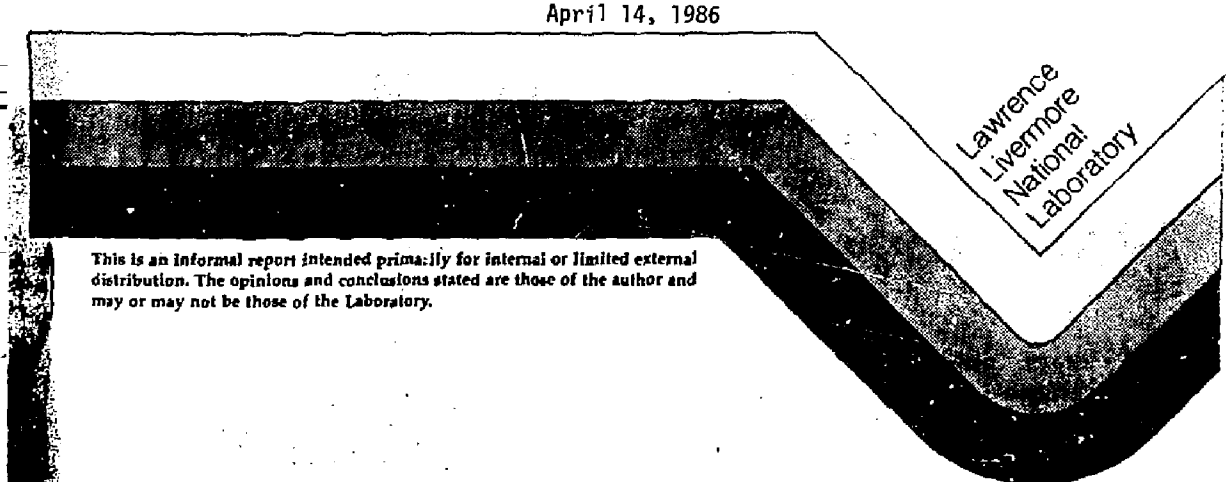

INDUCTION LINACS AS RADIATION PROCESSORS

Daniel L. Birx

Lawrence Livermore National Laboratory
University of California
Livermore, CA 94550

UCID--20785

April 14, 1986

DE86 015503

ABSTRACT

Experiments at the Lawrence Livermore National Laboratory (LLNL), University of California, in conjunction with the University of California at Davis have shown induction linear accelerators (linacs) to be suitable for radiation processing of food. Here we describe how it might be possible to optimize this technology developed for the Department of Defense to serve in radiation processing.

The possible advantages of accelerator-produced radiation over the use of radioisotopes include a tailor-made energy spectrum that can provide much deeper penetration and thereby better dose uniformity.

RADIATION PROCESSING

Considerable concern over ethylene dibromide (EDB) as a food processing technique has sparked a resurgence of interest in radiation processing.

Work performed jointly under the auspices of the U.S. Department of Energy by the Lawrence Livermore National Laboratory under contract No. W-7405-ENG-48 and for the Department of Defense under DARPA, ARPA Order No. 4395 and 5316, monitored by Naval Surface Weapons Center under document number N60921-85-POW0001; SDIO/BMD-ATC MIPR #W31-RPO-53-A127; and SDIO/NSWC reference number B00014-85-WR35514.

It has been known for some time that irradiation of food can kill pests and microorganisms within the food without damaging it or leaving harmful chemical residues. It has also been demonstrated that the shelf life is greatly extended in some cases. Conventional radiation processing is accomplished through exposure to radioisotopes such as ^{60}Co and ^{137}Cs.

It is the use of these radioisotopes rather than the process itself that appears to pose some of the major problems.

The gamma radiation produced by these sources is of too low an energy to provide good penetration into the food and, therefore, foodstuffs processed in this manner usually show large dose distributions between the exterior and interior. Another problem has been community acceptance of processing facilities containing large volumes of radioisotopes.

With this in mind we have embarked on a program to study the use of induction linear accelerators (linacs) as radiation sources. With these sources the energy spectrum of the produced radiation can be adjusted to give considerably enhanced penetration as compared to radioisotopes. It is also felt that accelerators tend to be more acceptable to the public than radioisotopes.

High-power induction linacs are currently undergoing extensive development as part of this country's Strategic Defense Initiative (SDI) program, primarily because induction linacs appear uniquely suited as a power source for the free-electron laser (FEL) amplifier. The FEL amplifier provides an efficient means to convert the energy possessed by an electron beam into electromagnetic radiation at power levels sufficiently high to make it useful as a surgical defensive weapon. The stringent requirements on the

induction linac dictated by this mission for efficient, reliable operation at high power levels should result in a device that more than satisfies the needs of a radiation processing application. When this came to the attention of the Laboratory directors and the University of California regents, a joint program was initiated to study further optimization of induction linacs to radiation processing.

INDUCTION LINACS AS FEL DRIVERS

The planned future 300-MeV induction linac for the optical-wavelength FEL amplifier program is modularized in 3-MeV sections. This accelerator has been designed to produce a 3-kA electron beam in 75-ns pulses at a repetition rate up to 5 kHz. Test modules have been constructed and are now undergoing extensive testing in the development laboratory.

The basic outline of a 3-MeV module presented in Fig. 1 shows a MAG-I-D nonlinear magnetic driver supplying power to two accelerator blocks, each containing ten accelerator cells operating at 150 kV. The inputs to these ferrite core cells correspond to the primary windings of a pulse transformer, while the multikiloampere electron beam comprises the secondary. As can be seen in Fig. 2, the primary windings are fed in parallel while the electron beam sees them in series adding up the incremental potentials.

In practice, things are not quite that simple, and requirements for solenoidal focusing, extraction of waste heat, and addition of compensation dictate a structure appearing more as the ten-cell block cutaway shown in Fig. 3.

INDUCTION LINACS

The major differences between the induction linac and a conventional radio-frequency standing wave accelerator are pointed out schematically in Fig. 4. The induction linac structure is nonresonant and, therefore, does not store energy. The electron beam current at an accelerating voltage must be adjusted to provide a match to the impedance of the drive lines for efficient operation. Energy that is not coupled into the electron beam cannot be stored and, therefore, must be dissipated as waste heat.

Realizable transmission line impedances are at most a few hundred ohms, and hence accelerating potentials of hundreds of kilovolts per cell specify electron beam currents in the thousands of amperes. The second stipulation results from the direct-current nature of the accelerating pulse. The duration of this pulse must be shorter than the time to saturate the ferrite accelerator cores. This time is simply dictated as

$$\int_0^{T_{pulse}} V \cdot dt \leq A \cdot \Delta B_s \quad ,$$

where V is the accelerating potential, A is the core cross-sectional area around which that potential appears, and ΔB_s is the available flux swing in the ferri(ferro)-magnetic core.

The geometry of an accelerator cell is further constrained by losses in the core material. These losses appear as a leakage current and must be small in comparison to the electron beam current for efficient operation. For an accelerator operating with a 75-ns pulse, the leakage current as a function of beampipe diameter and gradient is provided by Fig. 5. The preliminary

accelerator cell design for the radiation processor shown in Fig. 6 represents what we feel is a reasonable compromise between accelerator efficiency and length.

It is worth noting that this optimized operating point is a strong function of the accelerator pulse length. This effect is dramatized by Fig. 7. The choice of 75 ns is based on a compromise between the accelerator cells simplifying as the pulse length is decreased and the pulse power drive simplifying as the pulse length is increased. This position of the optimal operating point will most certainly be influenced by future technological improvements in both ferrite and the Metglas core material used in the magnetic pulse compressors.

The accelerator pulse-power drive is produced by nonlinear magnetic pulse compressors known as MAG-I-Ds. These three-stage pulse compressors are totally passive and rely only on the change in permeability of ferromagnetic materials as they saturate to provide a better than 60-fold temporal compression in energy and, thereby, a corresponding increase in power levels.

A simplified schematic for a MAG-I-D as well as an associated timing diagram are presented in Fig. 8. As each successive inductor saturates, its impedance is changed by a factor of $(\mu_{sat}/\mu_{unsat})^{1/2}$ and energy is transferred more and more rapidly down the chain.

The input charge time of 5 μsecs was chosen so that the power requirements at the input to the chain lies well within the performance curves of available thyratrons. The actual requirements on the thyratrons housed in the Intermediate Storage units are listed in Table 1.

Table 1. MAG-I-D intermediate storage requirements

Intrapulse parameters	
Pulse energy	910J
Operating voltage	25,000V
Storage capacitance	2.9μF
Charge storage	0.0725C
Discharge time	5μs
Charge time	150μs
I (peak)	29,000A
DI/DT (peak)	9,100A/μs
I (pulse average)	14,500A
At 1-kHz continuous-wave operation	
I (average)	72.5A
I (rms)	1,450A
Input power	910,000W

A cutaway of a MAG-I-D provided in Fig. 9 calls out the various stages and shows the inner construction. Throughout the assembly, unique cantilevered designs for the core windings eliminate solid dielectric supports and thus provide for complete recovery in the case of a dielectric failure. Freon is used as a dielectric fluid in the compression reactors and water in the energy storage devices. The Freon also removes heat generated in the

cores by anisotropy and eddy current losses. Estimates of the energy lost in the various compression stages during each pulse are shown in Fig. 10.

RADIATION PROCESSOR--FIRST GUESS

The basic parameters we have attempted to achieve in our radiation processor design are as follows. An energy of up to 10 MeV was chosen on the basis that operation at the current FDA-approved energy level of 5 MeV would always be a simple downscaling and that there is some indication that 10 MeV may be approved in the future. A power level in excess of 500 kW seemed desirable, and finally it was felt that every effort should be made to keep the design as close to the current FEL accelerator design as possible. It is doubtful that a food processing application will ever generate the R&D funding levels that are available in the SDI program, and we felt it was advantageous to make the best use of the technology developed for this purpose.

The above considerations led us to the design shown in simplified block diagram form by Fig. 11. The operating peak current in this case would be ~1 kA, and the entire accelerator could be driven by one MAG-I-O operating at 1 kHz. The overall efficiency of this accelerator is predicted by Fig. 12. Here what may be an excessive amount of energy is simply dissipated in $CuSO_4$ dummy loads in the compensation networks. These are present to provide pulse flatness for an improved waveshape and may be unnecessary.

The electron source is constructed from four accelerator cells in the first seven-cell block. A simplified cross section of this 0.6-MeV, 1-kA electron injector is shown in Fig. 13. The electron optics for this proposed injector have been optimized for achromaticity and can be seen in Fig. 14.

Achromaticity refers to the lack of dependence of the beam envelope and trajectory on energy. This is quite important in a high-power gun design because all components of the electron beam must transport through the accelerator or electrons incident on the beampipe may cause something to melt. It must be remembered that we are considering a pulsed accelerator where the voltage rise- and fall-time are a large fraction of the total pulse duration. During this rise and fall the electrons must still propagate through the accelerator. Computer calculations of the beam envelope at various energies are provided in Fig. 15.

EXPERIMENTS IN FOOD PROCESSING

During the past year experiments in conjunction between LLNL and the University of California at Davis have been performed at both sites. In these experiments a comparison was attenuated between the effects of accelerator-produced gamma radiation and ^{60}Co-sourced gamma radiation on food, insects, and bacteria. In these experiments the accelerator was adjusted to produce both the same average dose ratio and approximate energy as the ^{60}Co source at Davis.

There had been some concern that the large difference in duty factor between a continuous source and an extremely high peak dose ratio pulsed source might cause problems. To date no significant differences in the two treatments have been found.

CONCLUSIONS

An approach that would allow the use of electronically produced gamma radiation for processing has been discussed. While the relative merits over radioisotopic sources are somewhat controversial, and will be left to the reader to dwell on, it has been our attempt to show that a viable alternative does exist.

It should also be noted that while there was no discussion as to the suitability of radio-frequency accelerators for this application, this in no way implies that they could not be used for this purpose.

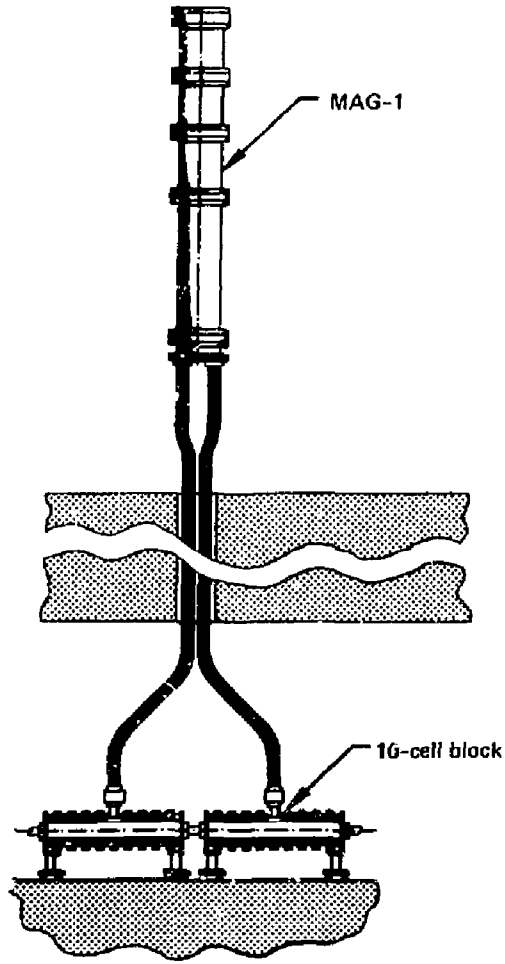

Figure 1. Schematic of 3-MeV FEL accelerator module.

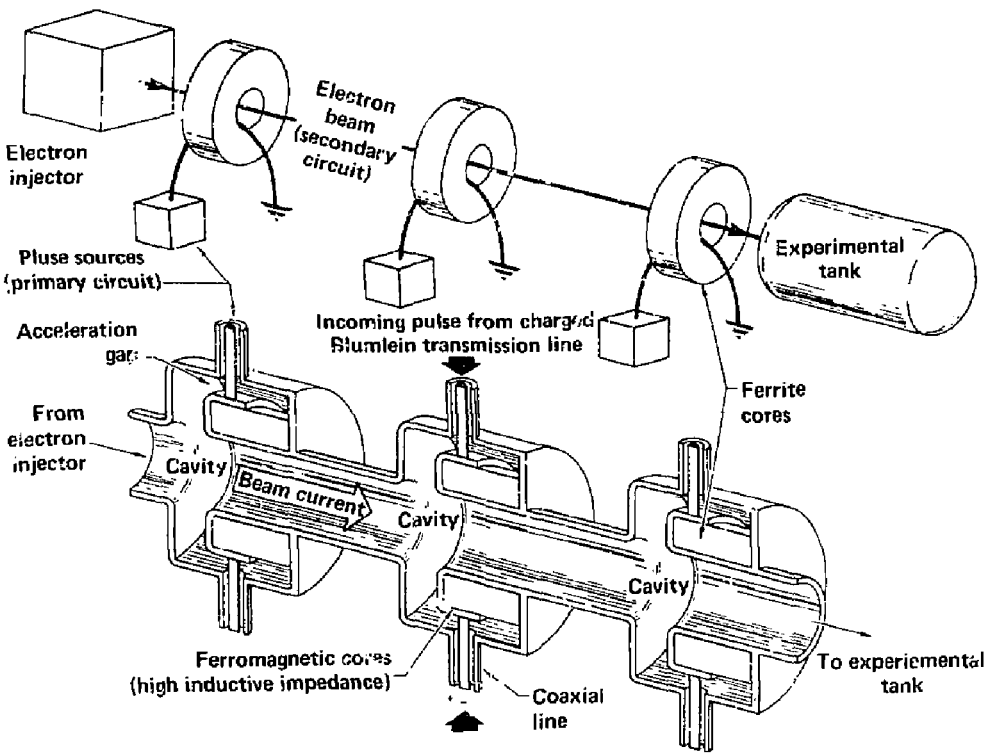

Figure 2. Operating principles of an induction linac, showing (a) a simplified schematic and (b) a cross section of an induction cell.

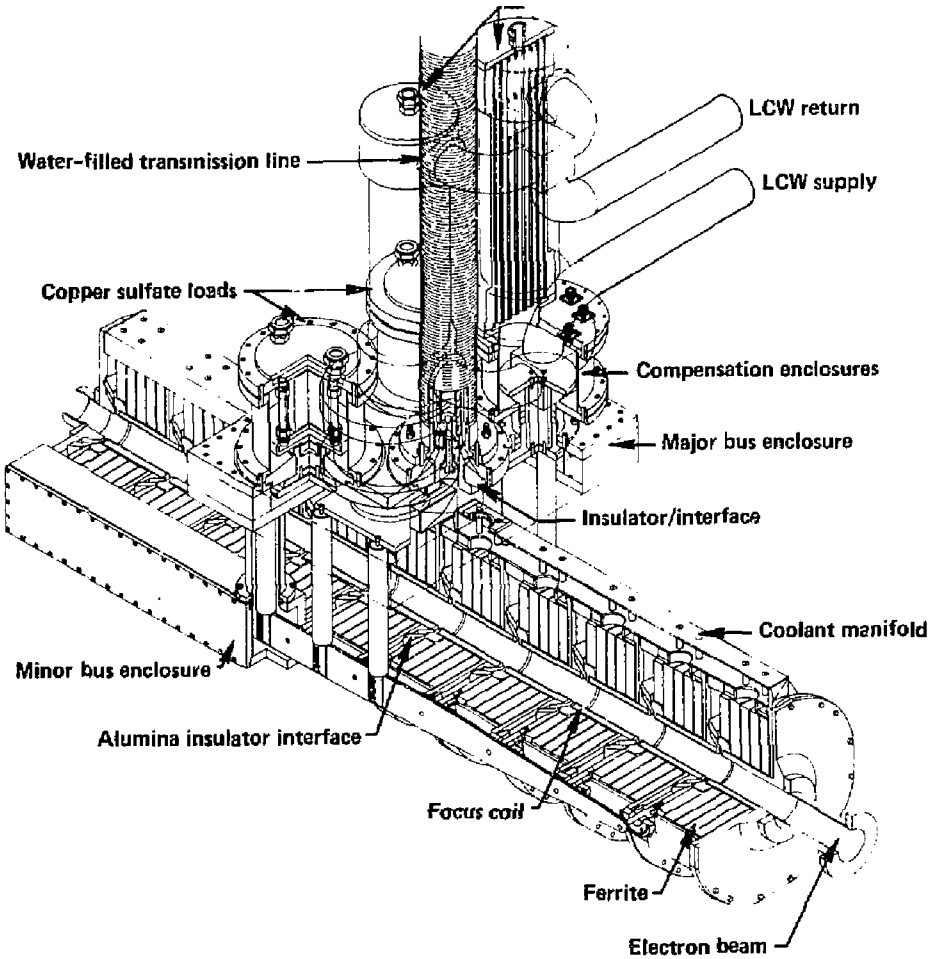

Figure 3. Cross section of possible 10-cell module.

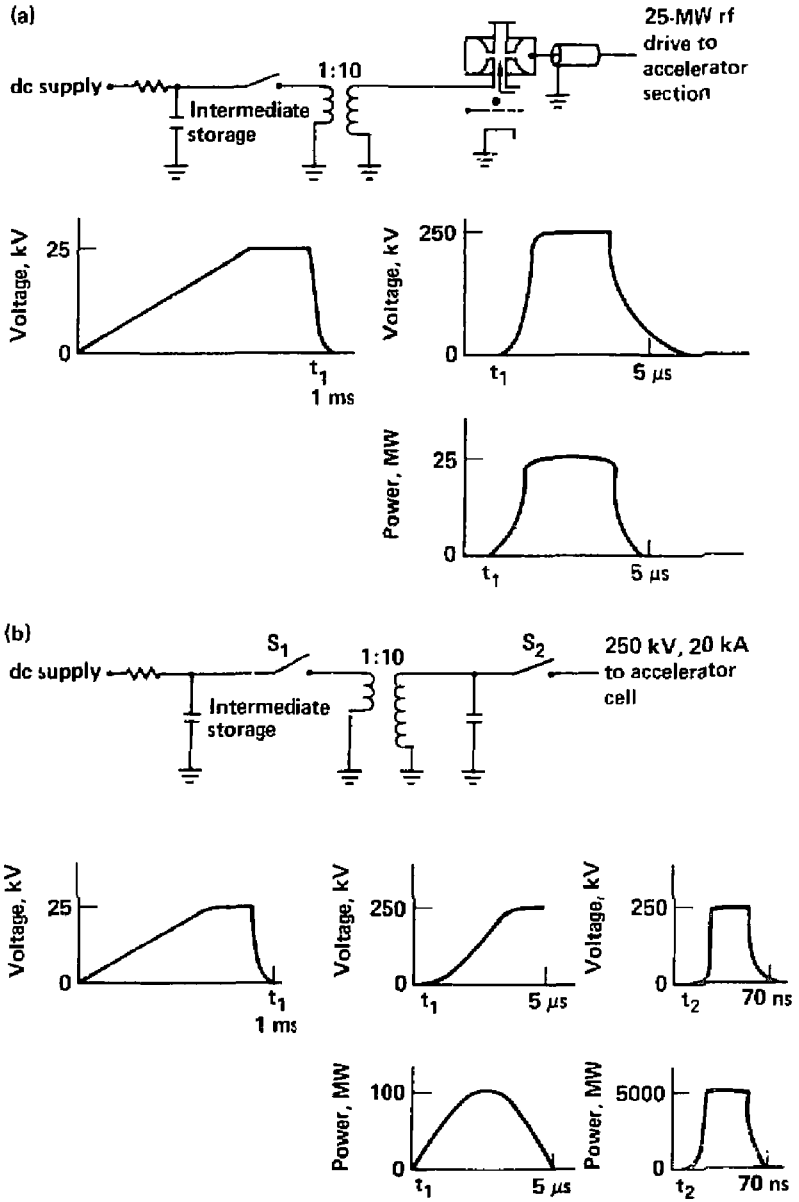

Figure 4. Comparison of accelerator pulsed-power requirements for (a) a linac and (b) an induction linac.

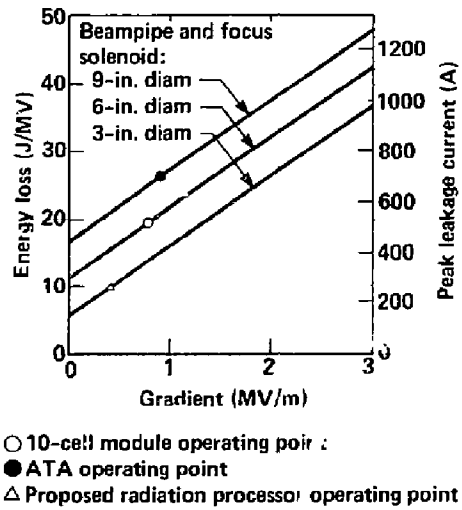

Figure 5. Leakage current as a function of beampipe diameter and gradient for an accelerator operating with a 75-ns pulse, a linear packing factor of 0.8, and TDK PE-11 core material.

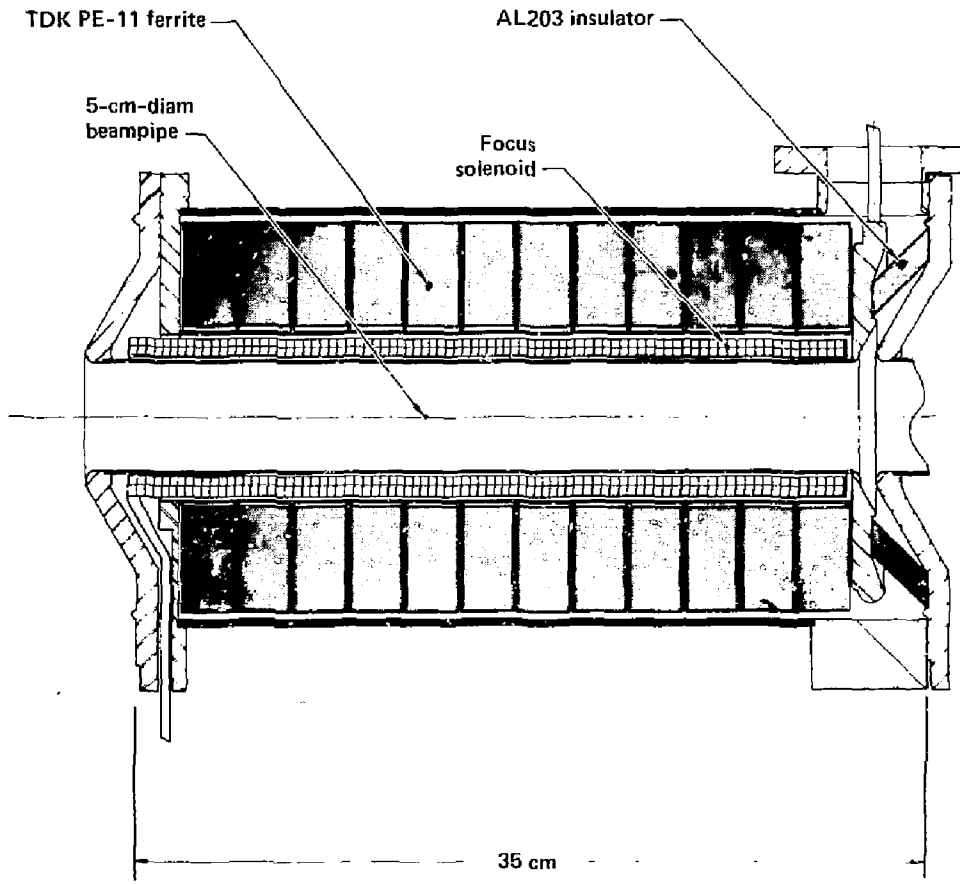

Figure 6. Preliminary accelerator cell design for a radiation processor.

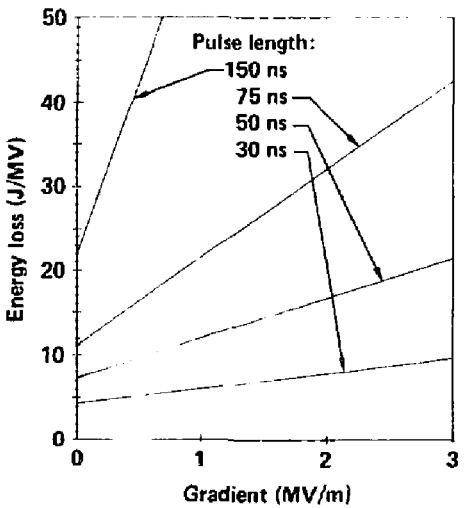

Figure 7. Energy loss versus gradient at different pulse lengths using a 6-in.-diam beampipe, a linear packing factor of 0.8, and TDK PE-11 core material.

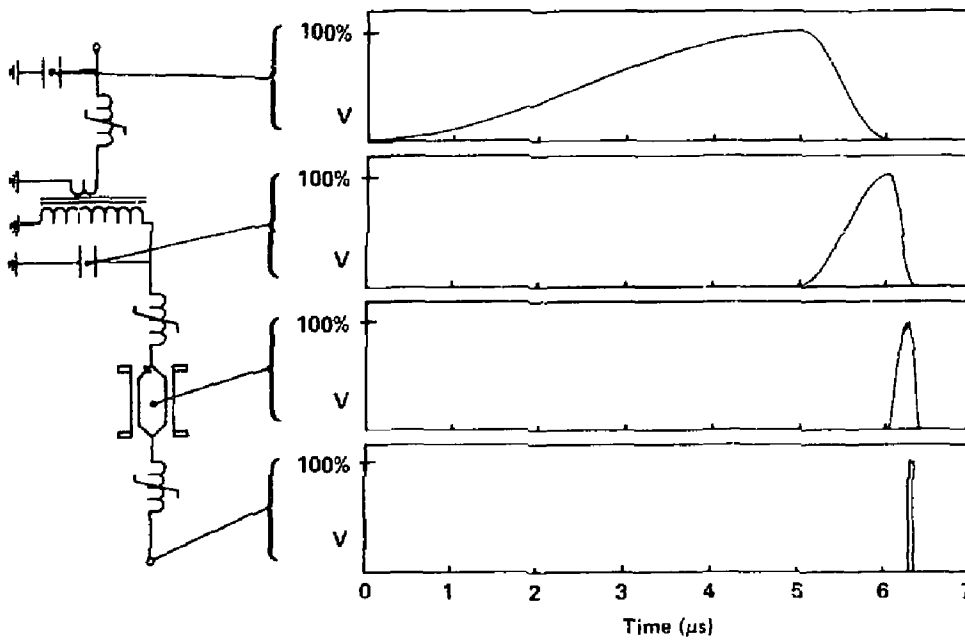

Figure 8. Pulse compression sequence for a MAG-I-D.

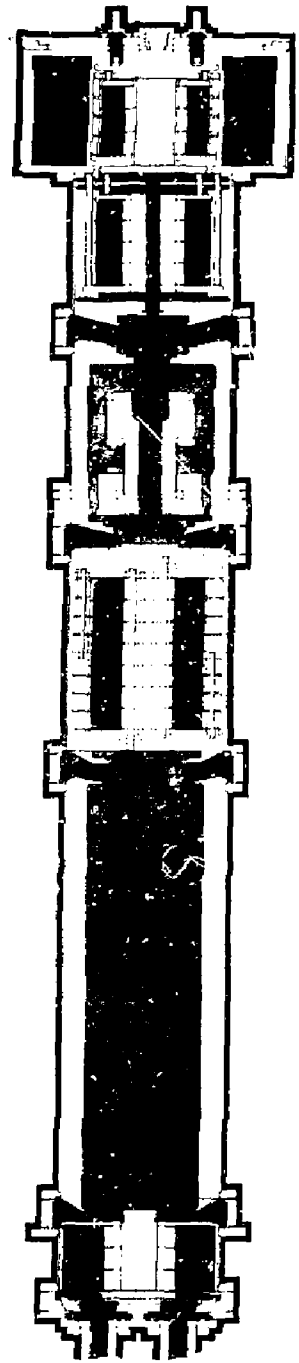

PRECOMPRESSION STAGE

1:10 STEP-UP TRANSFORMER

INTERFACE

1ST STAGE ENERGY STORAGE

INTERFACE

1 METRE

1ST STAGE COMPRESSION REACTOR

INTERFACE

2 OHM TRANSMISSION LINE

INTERFACE

OUTPUT STAGE COMPRESSION REACTOR

OUTPUT CABLE TRANSITION

4 OHM OUTPUT CABLE

MAG-I-D

Figure 9. Cutaway view of MAG-I-D.

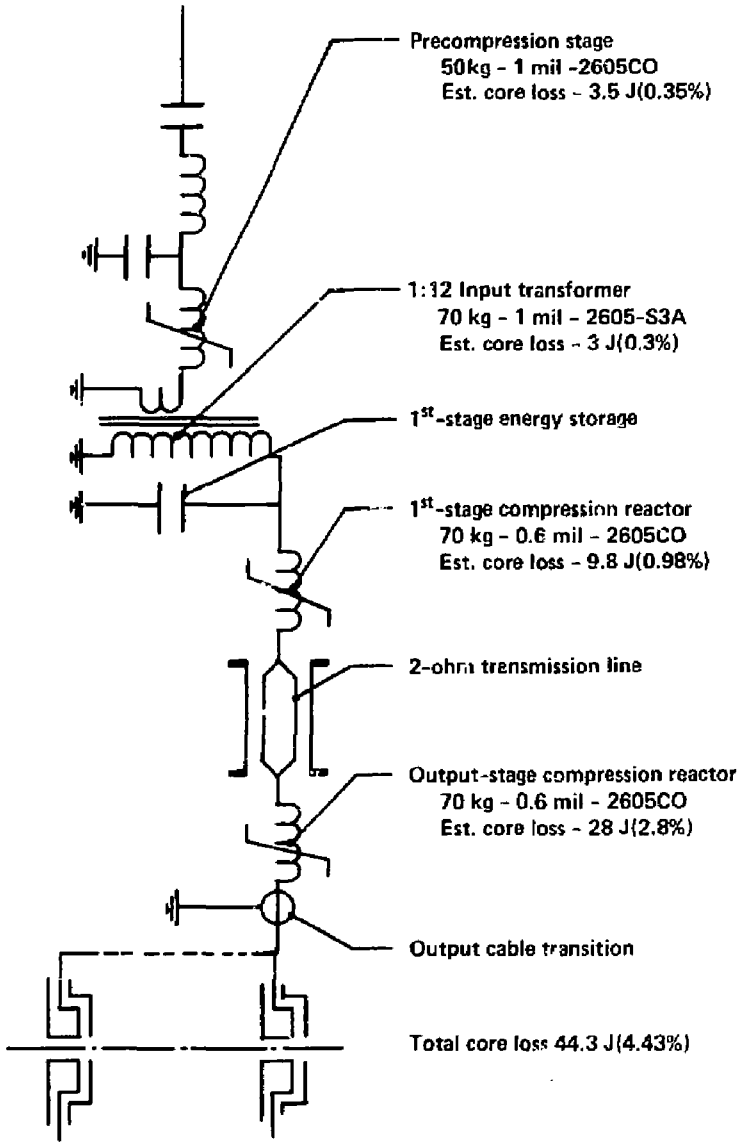

Figure 10. Estimated core losses per stage for MAG-I-D.

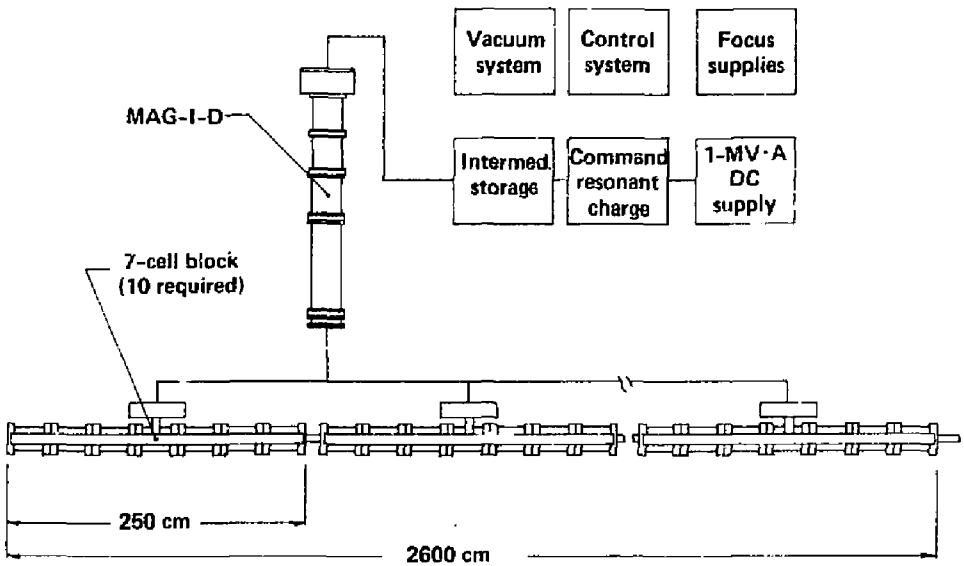

Figure 11. Simplified block diagram for a radiation processor: 10 MeV, 650 kW.

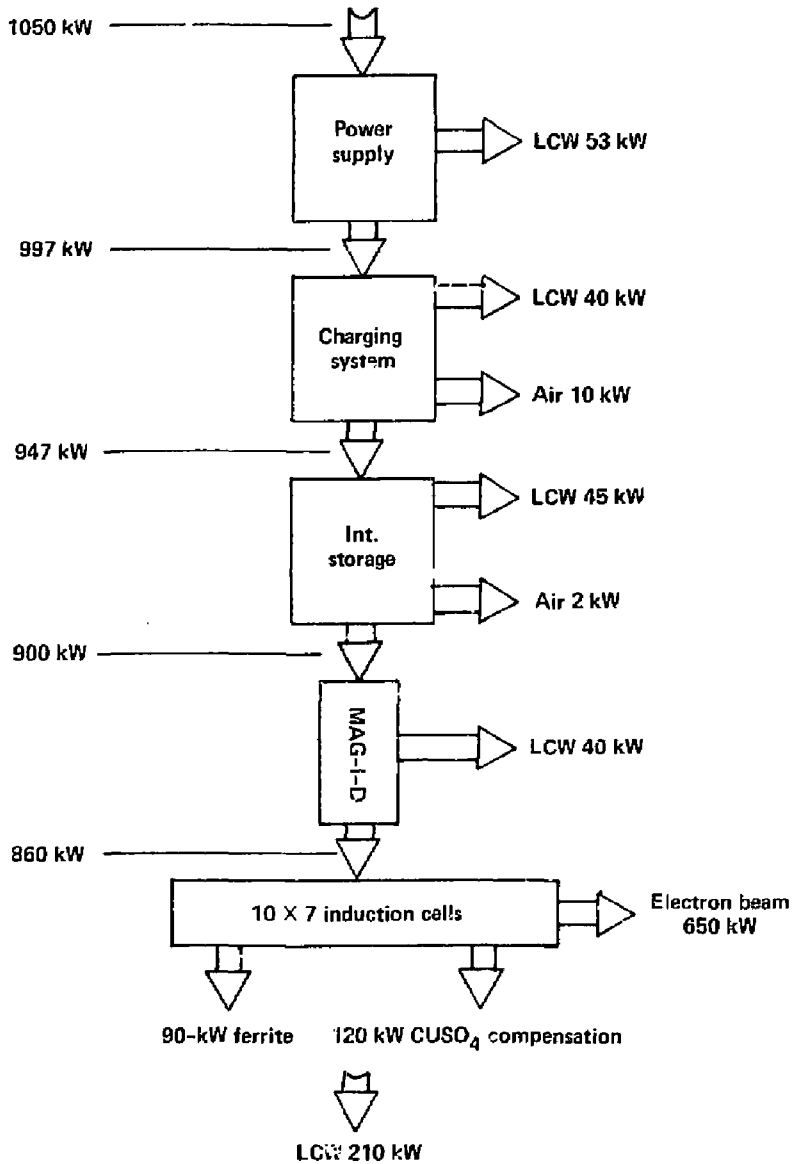

Figure 12. Predicted overall efficiency of the radiation processor shown in Fig. 11

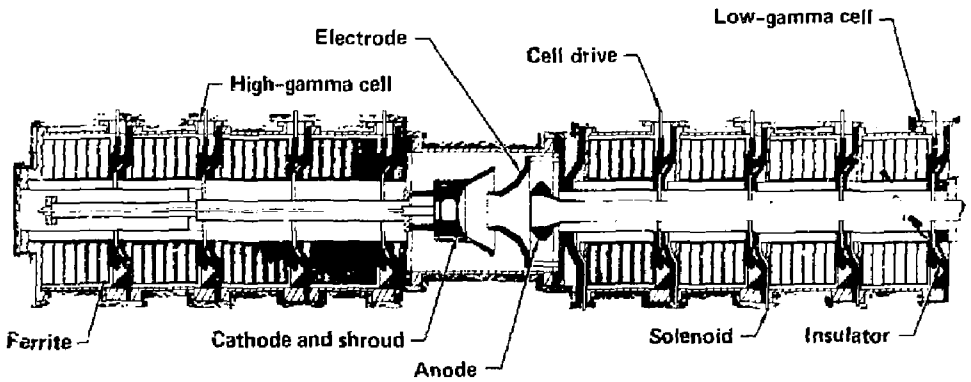

Figure 13. Preliminary design for high-power electron injector.

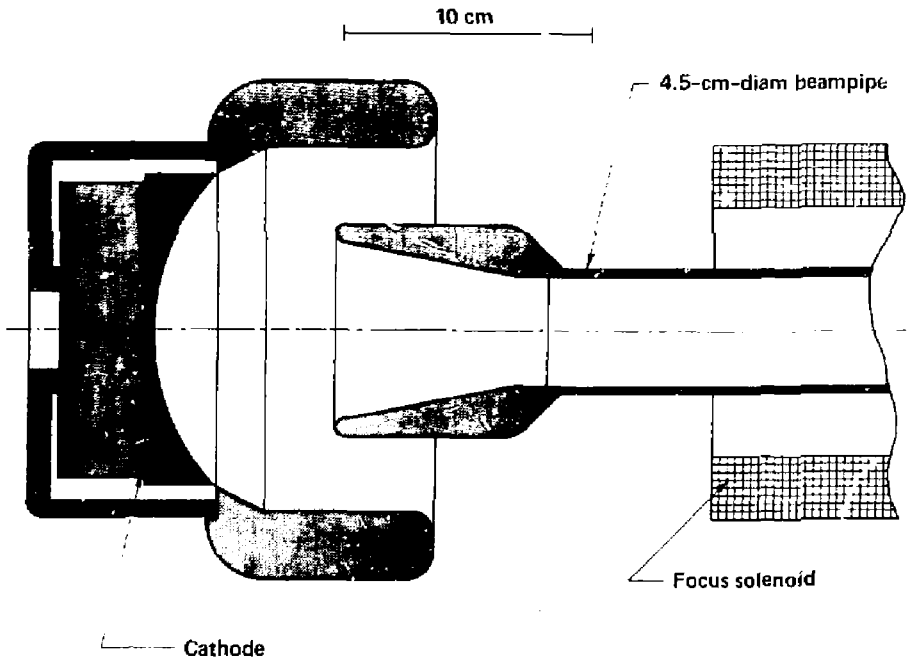

Design voltage - 0.6 MeV
Perveance - 2.26 UPERV
Design current - 1000 A
Focusing field - 300 Gauss on-axis
Cathode spherical radius - 9.21 cm
Cathode type - 12.7-cm-diam, M-type dispenser

Figure 14. Electron optics for a proposed electron-gun achromatic injector.

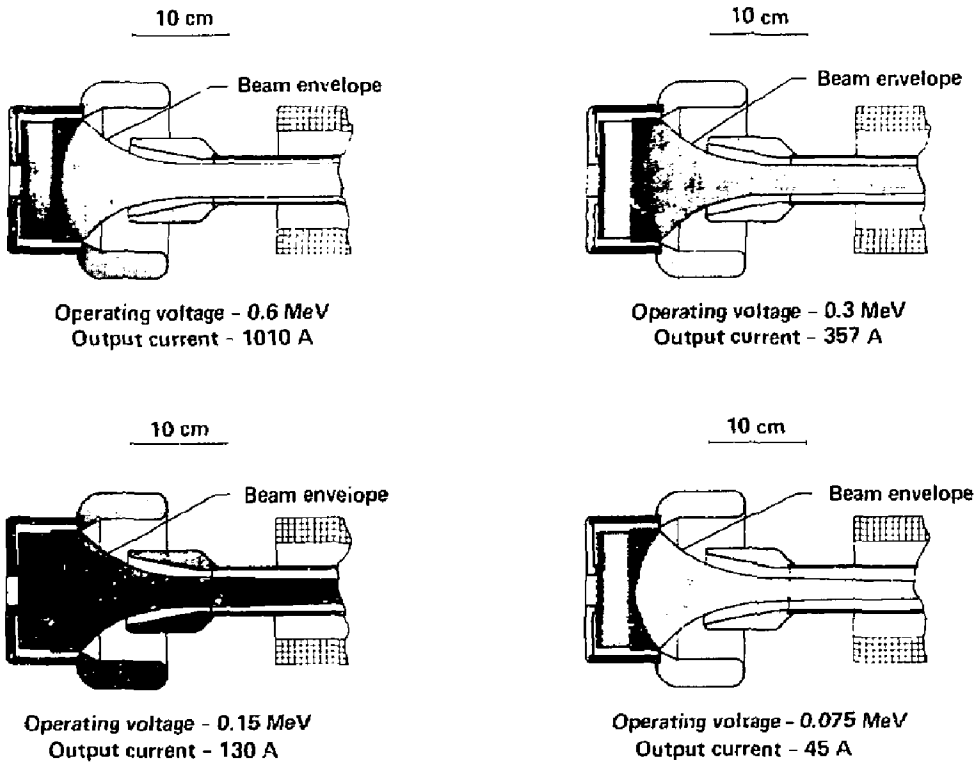

Figure 15. Computer calculations of the beam envelope at various energy levels for the achromatic injector.